Complex Composition Distribution of Poly(3-hydroxybutyrate-*co*-3-hydroxyvalerate)

Naoko Yoshie,* Hiroyuki Menju, Hidenori Sato, and Yoshio Inoue

Department of Biomolecular Engineering, Tokyo Institute of Technology, Nagatsuta, Midori-ku, Yokohama 226, Japan

Received May 8, 1995; Revised Manuscript Received July 3, 1995[⊗]

ABSTRACT: Four commercially available samples of bacterial poly(3-hydroxybutyrate-*co*-3-hydroxyvalerate) [P(3HB-*co*-3HV)] containing from 6.5 to 21.8 mol % 3HV have been fractionated by chloroform/*n*-heptane mixed solvent. They have been separated into several fractions with wide composition ranges. These results show that the composition distribution of as received bacterial P(3HB-*co*-3HV)s is extremely broad and/or has many peaks over a wide composition range. The effects of the complex composition distribution on physical properties have been analyzed through the comparison of melting and crystallization behavior between samples before and after fractionation. Three as received P(3HB-*co*-3HV)s show the behavior corresponding to the average composition in spite of their complex composition distribution. The melting temperature and spherulite growth rate correspond to the values expected from extrapolation of the data from the fractionated samples. In these copolyesters, cocrystallization of the chains within the wide composition range occurs. However, one as received P(3HB-*co*-3HV) has a higher melting temperature and faster growth rate than might be expected. The apparent crystallization behavior corresponds to that of P(3HB-*co*-3HV) with lower 3HV content. These data suggest that only the component chains of relatively low 3HV content are crystallized in this as received P(3HB-*co*-3HV). The crystallization of components of high 3HV content is significantly restricted. The extremely broad composition distribution of this copolyester affects the crystallization (melting) behavior.

Introduction

Poly(3-hydroxybutyrate-*co*-3-hydroxyvalerate) [P(3HB-*co*-3HV)] is a naturally occurring thermoplastic produced by bacteria.[1–3] There are many potential uses for this copolyester owing to its biodegradability and biocompatibility. A wide range of properties[4,5] were studied for this copolyester, such as melting temperature,[6–8] solid-state structure,[6,9,10–12] crystallization behavior,[11,13] mechanical properties,[14,15] and enzymatic degradation processes.[16] Most of these properties vary depending on the comonomer composition.

In general, synthesized polymers have composition distributions within a narrow range, meaning that all of the chains in a material have similar comonomer compositions. For bacterially synthesized copolymer, a narrow composition distribution has been also expected without careful consideration. However, we reported recently that some of bacterial P(3HB-*co*-3HV)s appear to be mixtures of several copolymers with different 3HV contents on the basis of ^{13}C NMR and DSC analysis.[17] Mitomo *et al.*[12] have fractionated P(3HB-*co*-45.7 mol % 3HV) and P(3HB-*co*-64.2 mol % 3HV) by a mixed solvent of acetone/water into several fractions. The properties of as received bacterial P(3HB-*co*-3HV) may be different from the "true" properties of P(3HB-*co*-3HV)s with narrow composition distributions. The composition distribution may affect various properties. It is important to know the composition distribution of as received P(3HB-*co*-3HV) and its effects on the physical properties of P(3HB-*co*-3HV).

In this paper, we attempt to make clear the complex composition distribution of bacterial P(3HB-*co*-3HV) and the effect of the distribution on physical properties. We carried out the fractional precipitation of four P(3HB-*co*-3HV) samples containing from 6.5 to 21.8 mol % 3HV by chloroform/*n*-heptane mixed solvent and obtained P(3HB-*co*-3HV) samples with narrow composition distributions. The thermal properties and crystallization behavior of these fractionated samples were compared with the as received unfractionated P(3HB-*co*-3HV) samples.

Experimental Section

The samples of P(3HB-*co*-6.5 mol % 3HV) and P(3HB-*co*-15.3 mol % 3HV) were provided by ICI (lot no.: PSM-17 and Po-16, respectively). The samples of P(3HB-*co*-19.4 mol % 3HV) and P(3HB-*co*-21.8 mol % 3HV) were purchased from Aldrich (lot no.: DM8231ML and HW06302PV, respectively).

Each P(3HB-*co*-3HV) sample was fractionated by the following procedure: 1 g of P(3HB-*co*-3HV) was first dissolved in chloroform at a concentration of 5 g·L^{-1}, and 10 mL aliquots of *n*-heptane were added until the solute was deposited. Then the solution was kept at room temperature for 24 h. The precipitate was separated from the solution by centrifugation and dried under vacuum at 60 °C for 48 h. The residue remaining in the supernatant solution was recovered by evaporation. The obtained residue was dissolved in chloroform at a concentration of 5 g·L^{-1}, followed by addition of *n*-heptane. These procedures were repeated until the addition of any amount of *n*-heptane caused no precipitation. The residue dissolved in solution with an excess amount of *n*-heptane was also recovered by evaporation.

Sample films for DSC and polarized microscopy were cast from 10 g·L^{-1} solutions in chloroform which were filtered onto glass Petri dishes. The solvent was allowed to evaporate for 2 days, and the resultant films were dried for 2 days under vacuum.

The 3HV contents of P(3HB-*co*-3HV) samples were determined by the relative intensities of the methyl resonances of 3HV and 3HB units in ^1H NMR spectra.[17] The *D* values of samples were determined by the analysis of the carbonyl resonance in ^{13}C NMR spectra.[17] The *D* value is defined as $D = F_{VV}F_{BB}/(F_{BV}F_{VB})$ where F_{XY} indicates the fractional population of the XY diad sequence. The carbonyl resonance splits into four peaks due to the diad sequence effects. The *D* value is estimated from the relative areas of these four peaks. The 270 MHz ^1H NMR spectra and the 67.9 MHz ^{13}C NMR spectra were obtained in $CDCl_3$ on a JEOL GSX-270 spectrometer.

Molecular weight was determined by a Toso HLC-8020 GPC system with a Toso SC-8010 controller and a refractive

[⊗] Abstract published in *Advance ACS Abstracts,* August 15, 1995.

0024-9297/95/2228-6516$09.00/0

Table 1. Fractionation of P(3HB-*co*-3HV)

	conc of *n*-heptane/%	yield/mg	3HV content/ mol %	M_n	M_w/M_n
P(3HB-*co*-6.5 mol % 3HV)[a]		1000	6.5	1.01×10^5	1.83
HV7-1	55.6	740	6.1	1.47×10^5	1.65
HV7-2	*b*	51	15.7	7.55×10^4	2.28
P(3HB-*co*-15.3 mol % 3HV)[a]		1000	15.3	8.01×10^4	1.70
HV15-1	50.0	64	10.9	*c*	*c*
HV15-2	55.8	421	11.3	7.50×10^4	1.92
HV15-3	72.5	167	18.5	1.19×10^5	1.42
HV15-4	69.4	191	25.3	4.92×10^4	1.75
HV15-5	*b*	53	*c*	1.02×10^4	1.46
P(3HB-*co*-19.4 mol % 3HV)[a]		1000	19.4	1.60×10^5	1.44
HV19-1	60.6	16	15.7	*c*	*c*
HV19-2	61.4	149	17.9	1.40×10^5	1.70
HV19-3	62.7	313	21.2	1.62×10^5	1.29
HV19-4	62.9	61	22.1	1.24×10^5	1.43
HV19-5	*b*	186	24.9	3.24×10^4	2.10
P(3HB-*co*-21.8 mol % 3HV)[a]		1000	21.8	2.06×10^5	1.80
HV22-1	51.7	18	10.2	2.06×10^5	2.27
HV22-2	56.9	195	13.3	1.63×10^5	1.95
HV22-3	56.8	171	17.8	1.60×10^5	1.88
HV22-4	61.4	99	18.8	2.25×10^5	1.68
HV22-5	63.8	92	22.6	2.14×10^5	1.50
HV22-6	67.7	134	28.6	9.99×10^4	1.50
HV22-7	*b*	108	34.4	3.80×10^4	1.54

[a] As received sample. [b] Residue remaining in the solution containing excess *n*-heptane. [c] Not determined.

detector with TSK gel G2000H_{XL} and GMH_{XL} columns. Chloroform was used as the eluant at a flow rate of 1.0 mL·min^{-1}, and the sample concentration was 0.5 g·L^{-1}. Polystyrene standards of low polydispersity were used to construct a calibration curve. GPC data were processed on a SC-8010 data processor to calculate the number average molecular weights (M_n) and polydispersity (M_w/M_n).

Thermograms were recorded using a Seiko DSC-20 equipped with a SSC-580 thermal controller. Film samples of 3−5 mg, which were sealed in aluminum pans, were first heated from room temperature to 195 °C at a heating rate of 10 °C·min^{-1}, followed by crystallization at 80 °C over 2 weeks. DSC thermograms were measured by heating from 80 to 200 °C at a heating rate of 10 °C·min^{-1}, unless otherwise indicated. The melting temperatures (T_m) shown in this paper are taken as the DSC peak position.

Measurements of the spherulite growth rates by polarized microscopy were carried out with an Olympus BX90 polarized microscope equipped with a Mettler FP82HT hot stage. Film samples were first heated from room temperature to 195 °C and then kept at 195 °C for 1 min. Subsequently, the samples were cooled to the crystallization temperature (T_c) and crystallized isothermally at T_c. The spherulite radius of all the samples increased linearly with time. Spherulite growth rates (G) were taken as the slope of the line obtained by plotting the spherulite radius as a function of time.

Results and Discussion

Fractionation of P(3HB-*co*-3HV). Bacterial P(3HB-*co*-3HV)s were fractionated into several samples by the precipitation using a mixed solvent of chloroform/*n*-heptane. The results of fractionation are shown in Table 1. The compositions of P(3HB-*co*-3HV) were determined by ^{1}H NMR spectroscopy.

The data shown in Table 1 indicate that the 3HV content of the fractionated P(3HB-*co*-3HV) gradually increases as the concentration of *n*-heptane in the solution increases. The molecular weights of the fractions are almost constant, with only the residue remaining in the solution with excess *n*-heptane having a smaller molecular weight. Therefore, only the difference in monomer composition caused the fractional precipitation by chloroform/*n*-heptane. As the side chain of 3HV is the ethyl group instead of the methyl group of 3HB, the polarity of the chain depends on the monomer composition. Therefore, when *n*-heptane is added to the solution in chloroform, P(3HB-*co*-3HV) is gradually precipitated in the order of the 3HV content.

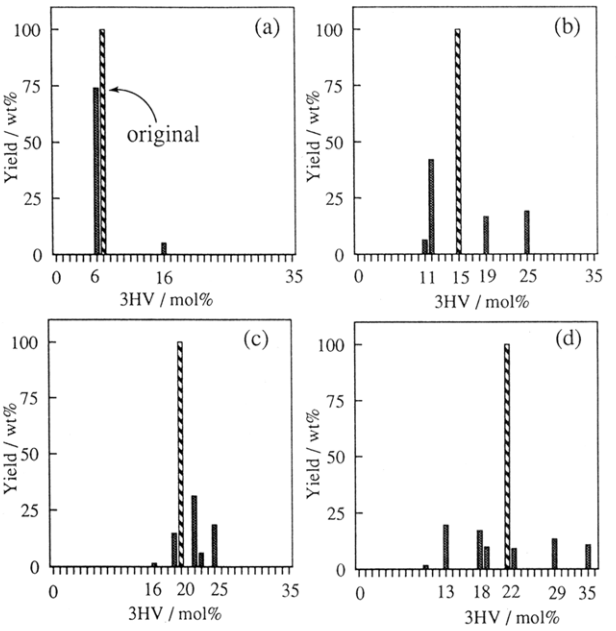

Figure 1. Relation between 3HV content and yield for fractions of (a) P(3HB-*co*-6.5 mol % 3HV), (b) P(3HB-*co*-15.3 mol % 3HV), (c) P(3HB-*co*-19.4 mol % 3HV), and (d) P(3HB-*co*-21.8 mol % 3HV). The column with the bold oblique line represents the original unfractionated sample.

The yields and the monomer compositions of fractionated samples represent the approximate composition distribution of the as received samples of bacterial P(3HB-*co*-3HV) (Figure 1). The composition of the four fractions from P(3HB-*co*-19.4 mol % 3HV) is spread from 18 to 25 mol % 3HV. Since the 3HV contents of the fractions are very close each other, this copolyester seems to have a broad composition distribution. P(3HB-*co*-6.5 mol % 3HV) has the composition distribution with two peaks, that is a large peak at 6 mol % 3HV and a small peak at 15 mol %. P(3HB-*co*-15.3 mol % 3HV) and P(3HB-*co*-21.8 mol % 3HV) have respectively three and five peaks with similar intensities. Since the 3HV contents of fractions are clearly different from each other, these copolyesters are likely to be mixtures of several copolymers with different 3HV contents. That is, these copolyesters have the composition distribution with several peaks. As a consequence, it is proved that as received bacterial P(3HB-*co*-3HV)s have broad composition distributions or composition distributions with many peaks.

In a previous paper,[17] we proposed a new parameter D defined as $D = F_{VV}F_{BB}/(F_{BV}F_{VB})$ to analyze the composition distribution. A statistically random copolymer has the D value being close to 1. The D value for a "blocky" copolymer is larger than 1. The term "blocky" indicates that the copolymer is a true block copolymer or a random copolymer having the composition distribution with many peaks. We have, however, found that this parameter is not very sensitive to the "blockiness", especially in the broad composition distributions. Although the bacterial P(3HB-*co*-3HV)s fractionated in this study have broad composition distributions or composition distributions with many peaks, the D values of these copolyesters are not large. The analysis

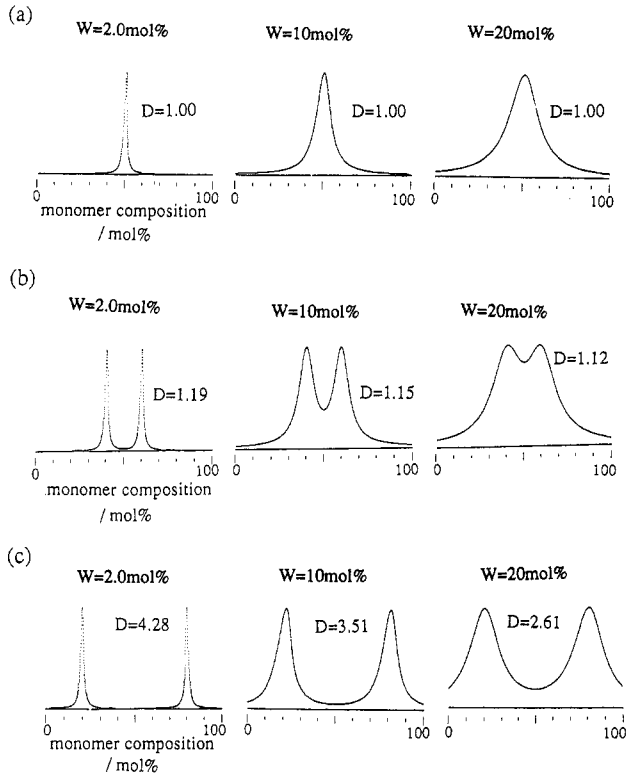

Figure 2. Schematic diagrams showing the relation between the composition distribution and the D value. Composition distributions are represented by (a) a Lorentz curve, (b) a sum of two Lorentz curves with peaks at 40 and 60 mol % 3HV, and (c) a sum of two Lorentz curves with peaks at 20 and 80 mol %. Half-height widths of peaks are indicated by W in mole percent.

of ^{13}C NMR spectra shows that the D values of the bacterial P(3HB-*co*-3HV)s containing 6.5, 15.3, 19.4, and 21.8 mol % 3HV are 1.14, 1.17, 0.994, and 1.46, respectively. Within experimental uncertainty in the measured diad fractions (±2−3 mol %), the D values of the as received P(3HB-*co*-3HV)s imply that these copolyesters are random copolymers. Although the D values were not analyzed for the fractionated samples, their D values were considered to be in the same range as the as received samples. The D value does not make it possible to discriminate the fractionated samples from as received ones.

Figure 2 explains the relation between the composition distribution and the D value. In this figure, we assume that (1) each component chain of an A/B copolymer has a random sequence and (2) the system of A/B copolymer chains has the composition distribution which is represented by a Lorentz curve or a sum of two Lorentz curves. The width of the Lorentz curve is represented by W in mol %. The average A/B composition of all the copolymers shown in Figure 2 is 50/50. Figure 2a shows the effect of the width of distribution on the D value. Although the width is varied from 1 to 20 mol %, the D value of each copolymer is 1.00 and not altered. The width of the distribution has little effect on the D value. Figure 2b shows the cases of composition distribution with two peaks at 40 and 60 mol %, where the width of distribution varied from 1 to 20 mol %. The D value is again close to 1 and not greatly varying. Even in the case where the peaks scarcely overlap (W = 1 mol %), the D value is no more than 1.19. The D values show the blockiness of a copolymer only when the two peaks are sufficiently far apart (Figure 2c).

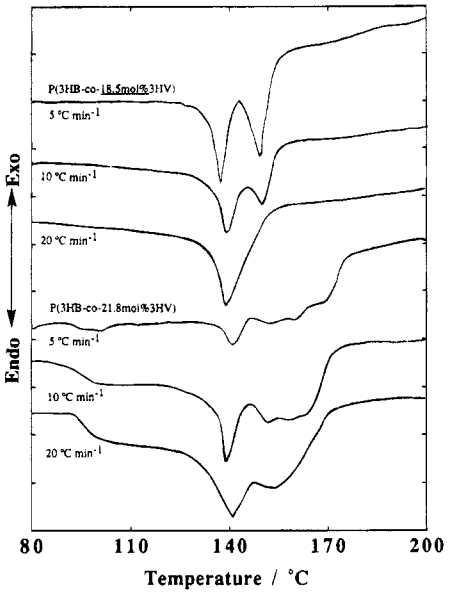

Figure 3. DSC thermograms obtained at various heating rates from P(3HB-*co*-21.8 mol % 3HV) and P(3HB-*co*-18.5 mol % 3HV).

Melting and Crystallization Behavior. Having concluded the complex composition distribution of the as received P(3HB-*co*-3HV)s, we now attempt to analyze the effects of the complex composition distribution of bacterial P(3HB-*co*-3HV) on its physical properties. Figure 3 shows the DSC thermograms obtained at various heating rates from P(3HB-18.5 mol % 3HV) and P(3HB-21.8 mol % 3HV). In order to make a clear distinction between the as received bacterial P(3HB-*co*-3HV)s and their fractionated samples, the fractionated samples are represented by the underlined 3HV content such as P(3HB-*co*-18.5 mol % 3HV). For all but the one thermogram obtained from P(3HB-*co*-18.5 mol % 3HV) at 20 °C·min^{-1}, multiple melting peaks were observed. When we interpret multiple melting peaks, we must distinguish between peaks arising from phase-separated structures and peaks arising from crystals rearranged during heating in the DSC. By simply varying the heating rate, these can be distinguished. In the case of P(3HB-*co*-18.5 mol % 3HV) (Figure 3a), the relative areas of two melting peaks vary considerably with heating rate. Such behavior is commonly observed for semicrystalline polymers and has been reported in P(3HB).[18] As the heating rate is increased, the higher temperature peak becomes small relative to the lower one; at the highest heating rate, the higher melting peak disappears. This result indicates that the lower temperature peak is the melting peak of crystals formed at T_c while the higher one is the melting peak of crystals recrystallized during the heating process in the DSC measurement. The true melting temperature of P(3HB-*co*-18.5 mol % 3HV) is given by the lower temperature peak. In the case of P(3HB-*co*-21.8 mol % 3HV) (Figure 3b), the variation of heating rate has little effecton the relative peak areas. Complex multiple melting is observed at every heating rate. This implies that some of the peaks are ascribable to the phase separation and the others to the recrystallization. More than two crystalline phases are formed in this copolyester. We, howver, cannot distinguish the effect of the phase separation from the effect of the recrystallization because of severe overlapping of the multiple peaks.

Figure 4 shows the DSC thermograms of P(3HB-*co*-3HV) samples at a heating rate of 10 °C·min^{-1}. All the

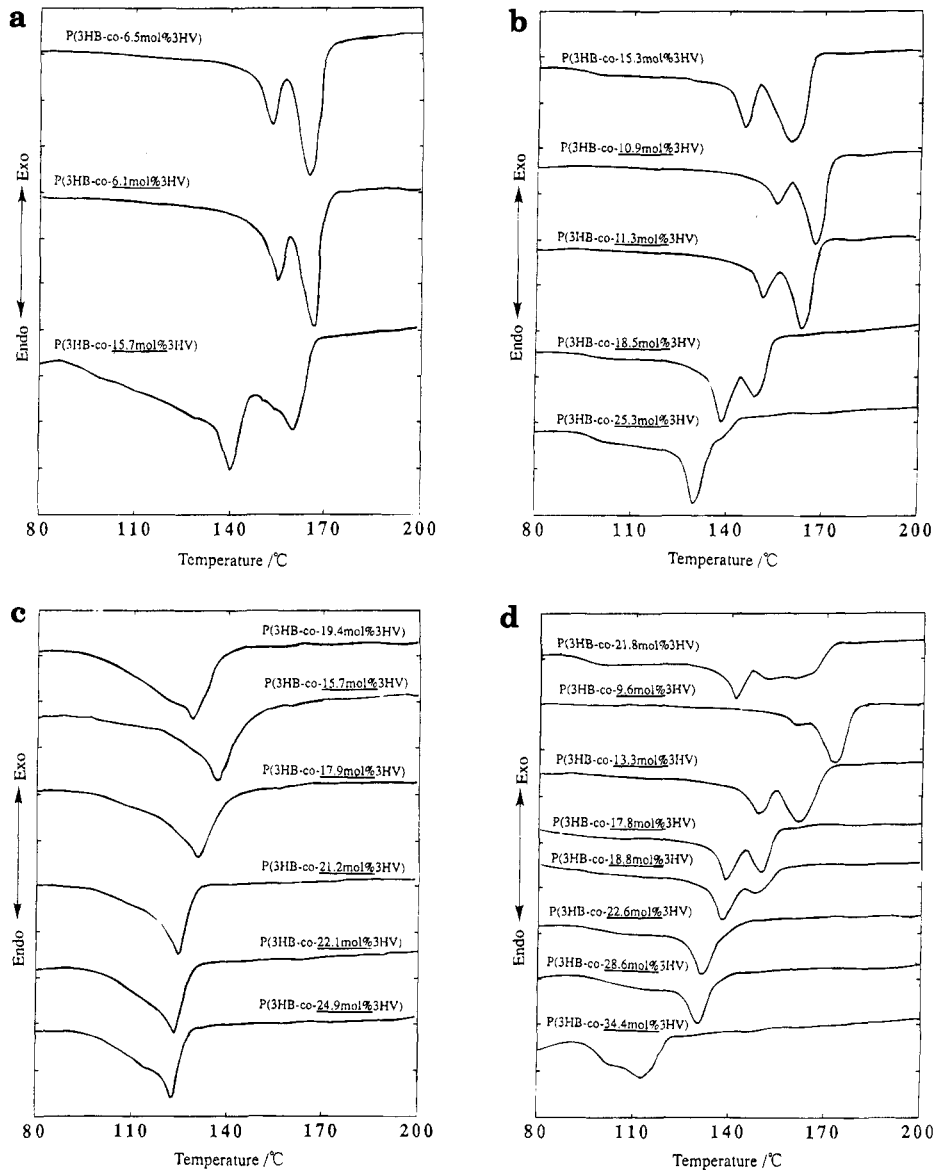

Figure 4. DSC thermograms for P(3HB-*co*-3HV)s before and after fractionation of (a) P(3HB-*co*-6.5 mol % 3HV), (b) P(3HB-*co*-15.3 mol % 3HV), (c) P(3HB-*co*-19.4 mol % 3HV), and (d) P(3HB-*co*-21.8 mol % 3HV).

fractionated samples have one or two sharp melting peaks. By varying the heating rate, it became evident that the two-peak behavior of the fractionated samples was ascribable to the recrystallization. The two-peak behavior of P(3HB-*co*-6.5 mol % 3HV) and P(3HB-*co*-15.3 mol % 3HV) is also ascribable to the recrystallization. In the case of P(3HB-*co*-21.8 mol % 3HV), more than two crystalline phases are formed, as mentioned above.

The T_m values of samples before and after fractionation are summarized in Figure 5. When a sample has two melting peaks, the lower temperature peak was taken as the melting peak of crystals. For P(3HB-*co*-21.8 mol % 3HV), the "true" T_m of each crystalline phase cannot be obtained from the DSC thermogram because of the overlapping of the multiple peaks. Only the apparent T_m values were determined from the peak tops. All the peak tops are plotted for this sample.

Three of the four as received P(3HB-*co*-3HV)s show behaviors corresponding to the average composition in spite of their complex composition distribution. The T_m of P(3HB-*co*-6.5 mol % 3HV) is similar to that of the main fraction, P(3HB-*co*-6.1 mol % 3HV). The T_m of P(3HB-*co*-19.4 mol % 3HV) is observed between those of P(3HB-*co*-17.9 mol % 3HV) and P(3HB-*co*-21.2 mol % 3HV). The T_m of P(3HB-*co*-15.3 mol % 3HV) is between those of P(3HB-*co*-11.3 mol % 3HV) and P(3HB-*co*-18.5 mol % 3HV). The T_m of these as received P(3HB-*co*-3HV)s coincides with the T_m expected from the extrapolation of the data from the fractionated samples.

On the other hand, the as received P(3HB-*co*-21.8 mol % 3HV) does not have the melting temperature expected from the average monomer composition. The apparent T_m values of P(3HB-*co*-21.8 mol % 3 HV), 143, 154, and 161 °C, correspond with the T_m values of P(3HB-*co*-9.6 mol % 3HV), P(3HB-*co*-13.3 mol % 3HV), and P(3HB-*co*-17.8 mol % 3HV), respectively. The thermogram of P(3HB-*co*-21.8 mol % 3HV) has no peaks in the temperature range expected from the average composition and also has no peaks in the range of melting of P(3HB-*co*-22.6 mol % 3HV), P(3HB-*co*-28.6 mol % 3HV), and P(3HB-*co*-34.4 mol % 3HV). This suggest that the partitioning of polymer chains occurs between the crystalline and amorphous phases. Only the chains with relatively low 3HV content enter the

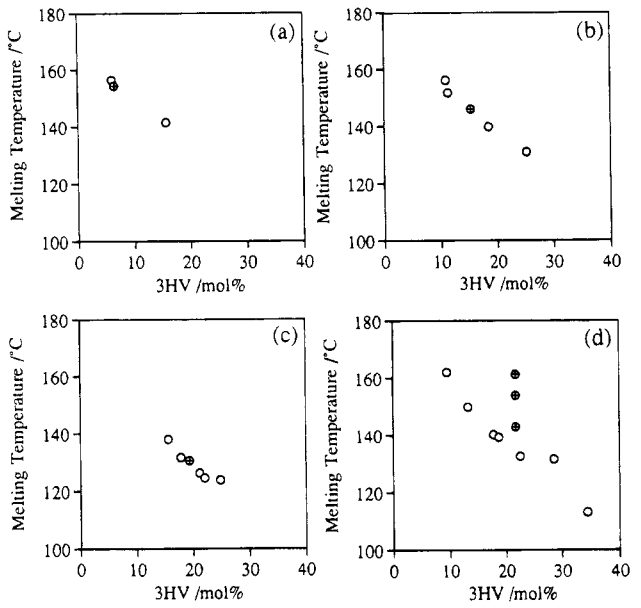

Figure 5. Melting temperature as a function of 3HV content for P(3HB-*co*-3HV)s before (⊕) and after (○) fractionation. P(3HB-*co*-3HV)s contain (a) 6.5 mol %, (b) 15.3 mol %, (c) 19.4 mol %, and (d) 21.8 mol % 3HV.

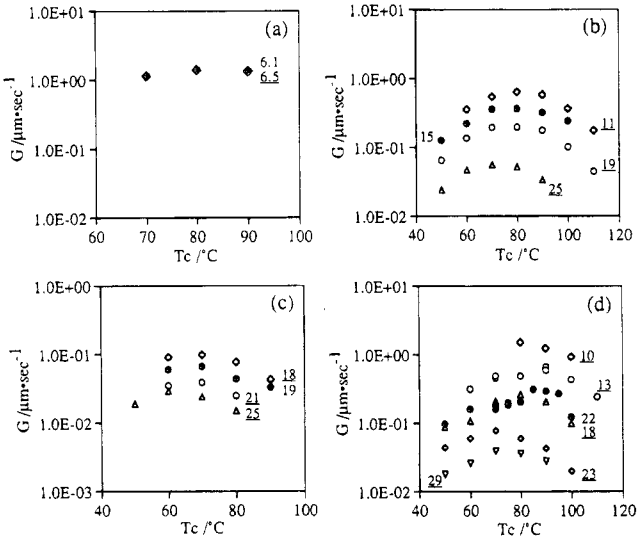

Figure 6. Spherulite growth rate as a function of crystallization temperature for P(3HB-*co*-3HV)s before (⊕) and after (◇, ○, △, ▽) fractionation. P(3HB-*co*-3HV)s contain (a) 6.5 mol %, (b) 15.3 mol %, (c) 19.4 mol %, and (d) 21.8 mol % 3HV. 3HV contents are shown as numbers besides symbols in mole percent. The underlined and nonunderlined contents indicate the contents before and after fractionation, respectively.

crystalline phase, and the chains containing much 3HV remain in the amorphous phase.

The spherulite growth rates were measured for the samples before and after fractionation. Volume-filling spherulites were formed at all crystallization temperatures investigated. The spherulite radius of all the samples increased linearly with time. Spherulite growth rates (G) were taken as the slope of the line obtained by plotting the spherulite radius as a function of time. Figure 6 shows spherulite growth rate (G) as a function of crystallization temperature (T_c).

The spherulite growth rates show the behavior similar to the melting temperature. The spherulite growth rate of P(3HB-*co*-6.5 mol % 3HV) is similar to that of its main fraction, P(3HB-*co*-6.1 mol % 3HV). The spherulite growth rates of P(3HB-*co*-15.3 mol % 3HV) and P(3HB-*co*-19.4 mol % 3HV) coincide with the rates expected from the average monomer composition. The complex composition distribution hardly affects the apparent behavior of crystallization (melting) for these copolyesters.

On the other hand, the spherulite growth of P(3HB-*co*-21.8 mol % 3HV) is markedly faster than that expected from the extrapolation of the average composition and close to that of P(3HB-*co*-17.8 mol % 3HV). This result also indicates the compositional partitioning between the crystalline and amorphous phases. It is noted that, in spite of the complex composition distribution, all the spherulites in a sample of P(3HB-*co*-21.8 mol % 3HV) have the same spherulite growth rate. This may be accounted for by assuming that the partitioning occurs at the growing front of the lamellae in a spherulite. That is, the chains of low 3HV content enter the lamellae while the chains containing many 3HV ejected into the interlamellar region. All the spherulites in a material have similar average monomer compositions, while the composition of the lamellae in a spherulite is different from that of the interlamellar amorphous region. The observation of three apparent peaks in the thermogram suggests that the compositions of every lamella are not the same in this copolyester. Lamellae with different compositions are formed.

It is know that the P(3HB-*co*-3HV) system exhibits isomorphism, that is, the cocrystallization of 3HB and 3HV units in a crystalline lattice.[6,9-12] The isomorphism between 3HB and 3HV units implies the possibility of the cocrystallization between P(3HB-*co*-3HV)s of different compositions. Actually, the cocrystallization has been reported between P(3HB) and P(3HB-*co*-3HV) of low 3HV content[19,20] and between P(3HV) and P(3HB-*co*-77 mol % 3HV).[21] The cocrystallization occurs when the difference in the composition is small. In P(3HV)/P(3HB-*co*-77 mol % 3HV),[21] only one sharp melting peak has been observed. The values of T_m and spherulite growth rate for this material are intermediate between those of P(3HV) and P(3HB-*co*-77 mol % 3HV). The width of the composition distributions of the as received copolyesters are indicated by the compositions of the fractionated samples. The range of the composition distributions for P(3HB-*co*-6.5 mol % 3HV), P(3HB-*co*-15.3 mol % 3HV), and P(3HB-*co*-19.4 mol % 3HV) are approximately 10, 14, and 9 mol %, respectively. These range is sufficiently small to exhibit the cocrystallization. The values of T_m and spherulite growth rate for as received P(3HB-*co*-3HV)s containing 6.5, 15.3, and 19.4 mol % 3HV are similar to those for P(3HV)/P(3HB-*co*-77 mol % 3HV). Therefore, it is concluded that the cocrystallization occurs in these as received P(3HB-*co*-3HV)s.

On the other hand, phase separation is observed for P(3HB-*co*-21.8 mol % 3HV). The compositions of the fractionated samples from this copolyester indicate that this material has the broadest composition distribution among the bacterial P(3HB-*co*-3HV)s investigated in this study. Its composition range is more than 20 mol %. It is well-known that crystallization kinetics of P(3HB-*co*-3HV) significantly depends on the composition.[11] The crystallization rate decreases as the 3HV content increases. The component chains of P(3HB-*co*-21.8 mol % 3HV) have various crystallization rates. The compositional partitioning of this copolyester is accounted for by assuming that only the chains with relatively fast crystallization rates enter the lamellae. The crystallization of the other chains is disturbed by

the lamellae formed previously. The extremely broad composition distribution affects the apparent crystallization (melting) behavior.

Further investigation of the effects of the complex composition on the crystallization is in progress through the blending of the fractionated P(3HB-*co*-3HV)s in our laboratory.

Acknowledgment. N.Y. is indebted to the Sumitomo Foundation for financial support.

References and Notes

(1) Holmes, P. A. *Phys. Technol.* **1985**, *16*, 32.
(2) Doi, Y.; Tamaki, A.; Kunioka, M.; Soga, M. *Appl. Microbiol. Biotechnol.* **1988**, *28*, 330.
(3) Doi, Y. *Microbial Polyesters*; VHC Publishers Inc.: New York, 1990.
(4) Barham, P. J.; Barker, P.; Organ, S. J. *FEMS Microbiol. Rev.* **1992**, *103*, 189.
(5) Inoue, Y.; Yoshie, N. *Prog. Polym. Sci.* **1992**, *17*, 571.
(6) Bluhm, T. L.; Hamer, G. K.; Marchessault, R. H.; Fyfe, C. A.; Veregin, R. P. *Macromolecules* **1986**, *19*, 2871.
(7) Kunioka, M.; Tamaki, A.; Doi, Y. *Macromolecules* **1989**, *22*, 694.
(8) Organ, S. J. *Polymer* **1993**, *34*, 2175.
(9) Kamiya, N.; Sakurai, M.; Inoue, Y.; Doi, Y. *Macromolecules* **1991**, *24*, 2178.
(10) Yoshie, N.; Sakurai, M.; Inoue, Y.; Chûjô, R. *Macromolecules* **1992**, *25*, 2046.
(11) Scandola, M.; Ceccorulli, G.; Pizzoli, M.; Gazzano, M. *Macromolecules* **1992**, *25*, 1405.
(12) Mitomo, H.; Morishita, N.; Doi, Y. *Macromolecules* **1993**, *26*, 5809.
(13) Organ, S. J.; Barham, P. J. *J. Mater. Sci.* **1991**, *26*, 1368.
(14) Bauer, H.; Owen, A. J. *Colloid Polym. Sci.* **1988**, *266*, 241.
(15) Scandola, M.; Ceccorulli, G.; Doi, Y. *Int. J. Biol. Macromol.* **1990**, *12*, 112.
(16) Doi, Y.; Kanesawa, Y.; Kunioka, M.; Saito, T. *Macromolecules* **1990**, *23*, 26.
(17) Kamiya, N.; Yamamoto, Y.; Inoue, Y.; Chûjô, R.; Doi, Y. *Macromolecules* **1989**, *22*, 1676.
(18) Organ, S. J.; Barham, P. J. *Polymer* **1993**, *34*, 2169.
(19) Organ, S. J.; Barham, P. J. *Polymer* **1993**, *34*, 459.
(20) Organ, S. J. *Polymer* **1994**, *35*, 86.
(21) Pearce, R. P.; Marchessault, R. H. *Macromolecules* **1994**, *27*, 3869.

MA9506039